TDA Progress Report 42-113

May 15, 1993

Precise Tracking of the Magellan and Pioneer Venus Orbiters by Same-Beam Interferometry—Part II: Orbit Determination Analysis

W. M. Folkner, J. S. Border, S. Nandi, and K. S. Zukor
Tracking Systems and Applications Section

A new radio metric positioning technique has demonstrated improved orbit determination accuracy for the Magellan and Pioneer Venus Orbiter orbiters. The new technique, known as Same-Beam Interferometry (SBI), is applicable to the positioning of multiple planetary rovers, landers, and orbiters which may simultaneously be observed in the same beamwidth of Earth-based radio antennas. Measurements of carrier phase are differenced between spacecraft and between receiving stations to determine the plane-of-sky components of the separation vector(s) between the spacecraft. The SBI measurements complement the information contained in line-of-sight Doppler measurements, leading to improved orbit determination accuracy. Orbit determination solutions have been obtained for a number of 48-hour data arcs using combinations of Doppler, differenced-Doppler, and SBI data acquired in the spring of 1991. Orbit determination accuracy is assessed by comparing orbit solutions from adjacent data arcs. The orbit solution differences are shown to agree with expected orbit determination uncertainties. The results from this demonstration show that the orbit determination accuracy for Magellan obtained by using Doppler plus SBI data is better than the accuracy achieved using Doppler plus differenced-Doppler by a factor of four and better than the accuracy achieved using only Doppler by a factor of eighteen. The orbit determination accuracy for Pioneer Venus Orbiter using Doppler plus SBI data is better than the accuracy using only Doppler data by 30 percent.

I. Introduction

Remote reconnaissance of planets in our solar system is conducted by NASA using unmanned space probes. A hyperbolic flyby of a planetary system may provide a few snapshots of geologic, atmospheric, and electromagnetic phenomena, which then reveal, through analyses, some understanding of the underlying physical processes which are taking place. A spacecraft placed in orbit about a distant planet, on the other hand, will provide a much longer time history of measurements of various phenomena, leading to more comprehensive physical understandings. Navigation is one of the many critical engineering functions necessary to support the planning and operations of space flight

missions. This article presents results of a flight demonstration of a new technique for improving navigation for planetary orbiters.

Radio antennas in the DSN provide communication links with distant spacecraft. Measurements of the microwave signal used for commanding the spacecraft and for relaying telemetry data from the spacecraft to Earth provide the basis for radio navigation. Any change in range between a Deep Space Station and a spacecraft affects the Doppler shift of the transmitted radio signal. Though many techniques, including ranging, radio interferometry, and onboard optical imaging, are used for interplanetary navigation, orbit determination for planetary orbiters has relied primarily upon Doppler data. The motion of an orbiter about a planet, induced by gravity, places a strong signature in the Doppler data received at Earth. Dynamic models allow the state of the orbiter relative to the central body to be estimated from a time history of the Doppler shift.

The accuracy of navigation solutions and the ability to project the spacecraft trajectory forward may directly impact the quality of the science return. Pointing, scheduling, and configuration of onboard instruments rely upon predictions of the spacecraft trajectory. Interpretation and registration of images and other measurements rely upon reconstruction of the spacecraft trajectory. Determination of harmonic coefficients of the planet's gravity field depends directly on the orbit determination accuracy. Improvements to navigation, such as reducing the volume of tracking time necessary to maintain a specified level of orbital accuracy, predicting a trajectory further ahead within a specified error tolerance, or improving the accuracy of the final reconstructed trajectory solution, can simplify operations and enhance the science return.

For a short-period (2–24 hr) planetary orbiter, the orientation of the orbit plane is the trajectory component least well determined by line-of-sight Doppler measurements. Doppler data acquired simultaneously at two widely spaced DSN stations, and then differenced, provide sensitivity to the orientation of the orbit plane [1]. Differenced-Doppler has been used operationally during the orbit phase of the Magellan mission to help meet stringent navigation requirements [2,3]. For the case when two spacecraft are in orbit about the same planet, an observable formed from Doppler measurements, differenced between stations and differenced between spacecraft, is expected to provide further improvements to navigation [4]. A demonstration of this technique using the Magellan and Pioneer Venus orbiters at Venus took place in the spring of 1991. A detailed discussion of the data acquisition and measurement error analysis has been given earlier [5].

In 1991 the Pioneer Venus Orbiter (PVO) spacecraft, launched in 1978, was in a highly eccentric orbit about Venus with a period of about 24 hours. The Magellan spacecraft joined PVO in orbit around Venus on August 10, 1990. During 1991, Magellan was in a less eccentric orbit with a period of about 3.26 hours. Same-Beam Interferometry (SBI) data sets were acquired in February and April 1991. Orbit determination solutions from these data sets have been obtained using various combinations of Doppler, differenced-Doppler, and SBI data. Formal errors associated with the solutions and solution comparisons for adjacent data arcs are examined to assess orbit determination accuracy. An overview of the simultaneous tracking technique is presented below, followed by discussions of the data scheduling, orbit determination strategy, and orbit determination results.

II. Radio Metric Measurements

Three types of radio metric measurements were included in this demonstration: two-way Doppler, differenced-Doppler, and SBI. Two-way Doppler is collected for a single spacecraft from a single Deep Space Station. Differenced-Doppler is collected by two widely separated Deep Space Stations for a single spacecraft. SBI is collected for two spacecraft simultaneously at two widely separated Deep Space Stations. The DSN Deep Space Stations used are located in California, Australia, and Spain.

Two-way Doppler (referred to below as Doppler) is collected when the Deep Space Station sends a stable carrier signal to the spacecraft and the spacecraft replies with a signal phase-locked to the uplinked signal. The frequency shift of the signal received by the Deep Space Station compared to the transmitted signal provides a measure of the rate of change of range to the spacecraft. The DSN currently tracks planetary orbiters at either S-band (2.3 GHz) or at X-band (8.4 GHz). During the time of interest for this demonstration, most of the Magellan Doppler data acquired were derived from the station transmitting and receiving signals at X-band while PVO data were derived from a station transmitting and receiving a signal at S-band. For Doppler at S-band, the intrinsic data accuracy is limited by solar charged particle fluctuations to about 1.0 mm/sec for the inferred range-rate for a 60-sec averaging time. For data taken at X-band, the accuracy is also limited by solar charged particle fluctuations, but at a reduced level. The X-band Doppler intrinsic data accuracy is typically about 0.1 mm/sec for the inferred range-rate for a 60-sec averaging time.

Differenced-Doppler data are collected when the spacecraft carrier signal is measured at two Deep Space Stations.

The difference in the received carrier frequencies provides a measure of the difference in the range-rate from each Deep Space Station to the spacecraft. One component of the spacecraft velocity in the plane normal to the line-of-sight (plane of the sky) is inferred from this difference in line-of-sight range-rate, namely the component in the direction of the vector separating the two Deep Space Stations projected onto the plane of the sky. The intrinsic accuracy of X-band differenced-Doppler is typically 0.05 mm/sec for the inferred differenced line-of-sight range-rate for a 60-sec averaging time. Accuracy is improved relative to Doppler because station differencing reduces the effect of solar plasma fluctuations by removing fluctuations common to the two downlink ray paths. The accuracy with which the plane of sky velocity component is inferred is approximately the differenced range-rate accuracy times the ratio of the Earth–spacecraft distance to the distance between the two Deep Space Stations.

The SBI measurement of two spacecraft is depicted in Fig. 1. The two spacecraft in orbit about the same planet are so close angularly, as seen from Earth, that they may be observed in the same beamwidth of an Earth-based radio antenna. Each spacecraft carrier signal phase is recorded by two widely separated Deep Space Stations. Differencing the received carrier phases, first between stations and then between spacecraft, gives a measure of the separation of the two spacecraft in the plane of the sky along the projected baseline. The phase difference can be ambiguous by an integer number of cycles; the ambiguity must be resolved by a priori information (such as a sufficiently precise Doppler-only orbit) or by estimating a phase bias parameter for each SBI data arc. SBI data were taken at S-band for this orbit determination demonstration since PVO was tracked at S-band and Magellan was transmitting low-rate data at S-band in addition to the primary X-band signal. The SBI data accuracy corresponded to a doubly-differenced range accuracy of 1.5 mm for 5-min integration times [5]. From this doubly-differenced phase the separation of the two spacecraft in the plane of the sky can be inferred with an angular accuracy of 180 prad for a baseline length of 8000 km (which is an average length of the separation vector between antennas from different DSN complexes projected onto the plane normal to the Earth–spacecraft direction). At a distance of 1.5 astronomical units (AU's), the SBI data accuracy corresponds to a spacecraft-separation measurement accuracy of 40 m. X-band data are expected to be more accurate by an order of magnitude due to reduced sensitivity to solar charged particle fluctuations.

All of the radio signals are affected by delays due to Earth ionosphere and troposphere as well as delays due to solar plasma. Calibrations for the troposphere were applied based on a seasonal model [6]. Calibrations for the Earth's ionosphere were applied based on daily measurements from Earth-orbiting beacon satellites [7].

III. Estimation Models

The spacecraft trajectory was integrated from initial position and velocity conditions (epoch state) using models for the dynamic forces on the spacecraft. The largest force was due to the gravitational field of Venus, which was modeled as a point mass (gravitational mass [GM]) term and potential field composed of spherical harmonic terms to degree and order 21 estimated from several years of radio metric data for PVO and Magellan [8]. Other significant forces were due to solar pressure, the solar point mass perturbation and, for Magellan, atmospheric drag and momentum wheel desaturation thrusts which occur twice daily. The right ascension and declination of the Venus spin axis and the rotation period were derived from Magellan radar images of surface features [9]. The rotation angle of Venus about the spin axis at a reference epoch was estimated for this demonstration from a 10-day arc of PVO and Magellan Doppler data.

The Deep Space Station locations were mapped from Earth-fixed locations to inertial space using models for precession, nutation, and solid Earth tides, and calibrations for polar motion and length of day variations. Computed values for measurements were derived from nominal values for the spacecraft epoch state, force models, and inertial Deep Space Station locations. A least-squares fit to the observations minus the computed measurements was made to estimate model parameters. For this demonstration, gravity field parameters were not adjusted since, for short data arcs, epoch state errors can be aliased into gravity field parameters. The uncertainties in the spacecraft trajectory caused by imperfect unadjusted model parameters were included through the use of consider analysis [10]. The derived uncertainty in the trajectories depends on the formal error covariance for the solved-for parameters (computed) and on the uncertainty assumed a priori of the unadjusted (considered) parameters.

For short data arcs, the spacecraft trajectory uncertainty is usually dominated by the uncertainty in the unadjusted gravity field. Because of this, the optimal orbit determination solution may not be achieved by weighting all of the data at its intrinsic accuracy since the estimated epoch state is derived by neglecting the considered parameters. By neglecting the gravity field, the estimation filter will produce a solution based on an over-optimistic estimate for the spacecraft plane-of-sky velocity based on the Doppler data. Without taking this into account in some

manner the differential data types may not fully influence the solution. The effect of mismodeling can be reduced by deweighting the Doppler data and including differential data, weighted at its intrinsic accuracy, in the estimation. This strategy has been used in the operational navigation for Magellan [2,3].

IV. Data Arcs

During the spring of 1991, Magellan was conducting radar mapping operations. Magellan typically performed radar mapping for one hour of each orbit, during which there was no signal transmitted to Earth. Radio metric data could be collected for Magellan during the two hours of telemetry playback each orbit. For the same time period, PVO was in an orbit with a period of 24 hours. S-band Doppler data from PVO were collected for approximately 6 hours per day centered roughly about periapsis, which occurred during the California–Australia visibility period. SBI data were acquired over an eight-day period beginning February 16, 1991, and over a ten-day period beginning April 6, 1991. Figures 2 and 3 show the orbits of the two spacecraft as viewed from Earth for these two time periods. Nominal orbital elements for the spacecraft are given with respect to the plane of the sky in Tables 1 and 2.

For the SBI demonstration, data could be acquired only when both Magellan and PVO were transmitting to Earth and when stations were allocated at two DSN complexes. Because Magellan used differenced-Doppler operationally, stations from different DSN complexes were scheduled to simultaneously track Magellan for about five hours during each 48-hour period. SBI data could then be acquired at those stations, on a non-interference basis, when PVO was also transmitting. This scheduling resulted in an average of two hours of SBI data acquired every other day. One SBI bias parameter was needed for each hour of SBI data since the Magellan signal was interrupted by either a mapping cycle or an attitude calibration after each hour of telemetry.

Because of the sparseness of the SBI and PVO Doppler data, 48-hour non-overlapping data arcs were chosen for orbit determination solutions. A typical data schedule for a 48-hour data arc is shown in Fig. 4. Each of the data arcs contained approximately 13 orbits of Doppler data from Magellan, about 5 hours of differenced-Doppler for Magellan, and Doppler from two PVO orbits, each with about 6 hours of data centered about periapsis.

Four two-day data arcs were formed for the period February 14 to February 22, 1991, as summarized in Table 3. Since no Doppler data were collected from PVO for the orbit beginning on February 14, 1991, Doppler data from the previous orbit were included to allow each solution to contain data from two PVO orbits. PVO Doppler data within 1 hour of periapsis were excluded to reduce sensitivity to gravity field mismodeling. SBI data were acquired on the California–Australia baseline near the time of PVO periapsis. Five data arcs were formed from data acquired from April 6 to April 16, 1991, as summarized in Table 4. Most of the SBI data acquired in April were during the California–Australia overlap period with some data also acquired from the California–Spain baseline.

V. Orbit Determination Strategy

For this demonstration, orbit solutions for each spacecraft were formed for each data arc using different combinations of data. Three combinations of data were used for Magellan: Doppler only, Doppler plus differenced-Doppler, and Doppler plus SBI. Solutions for PVO were formed using only Doppler data and using Doppler plus SBI data. Orbit determination accuracy was assessed by comparing the orbit solutions for adjacent data arcs. To do this, the orbit solution from each data arc was propagated forward to the first orbit in the succeeding data arc and differenced with the succeeding solution trajectory. This solution-to-solution consistency provides one measure of orbit determination accuracy for post-fit data analysis. Orbit prediction, while of interest for mission operations, is not addressed here because neither experiment (February 1991 or April 1991) was long enough to provide more than one or two orbit prediction comparisons for prediction times of approximately one week (which is the typical period of interest).

The quantities estimated for each data arc were six epoch-state parameters for each spacecraft, an atmospheric drag coefficient for Magellan, and phase biases for the SBI data. The epoch for each spacecraft was chosen to be an apoapsis near the beginning of the 48-hour data arc. A priori uncertainties for the estimated state and phase bias parameters were very large so as not to significantly constrain the solution. The a priori uncertainty for the Magellan atmospheric drag was 100 percent of its nominal value; this uncertainty is consistent with variations in the Venus atmospheric density above 100 km [11]. (Because the gravity field is mismodeled and no gravity field corrections were estimated, the estimated atmospheric drag tended to absorb gravity field mismodeling and hence not represent the actual atmospheric drag. This estimation of atmospheric drag is used here to allow comparison with other Magellan orbit determination solutions [2,3].)

The data weights used in the solutions varied depending on which combinations of data were used. The intrinsic

accuracies of the data for a 60-sec sampling time were assumed to be 0.1 mm/sec for the Magellan X-band Doppler data, 1 mm/sec for the S-band PVO Doppler data, and 0.05 mm/sec for the Magellan X-band differenced-Doppler data. The accuracy of the SBI data was 1.5 mm for 5-min averaging times. When fitting only Doppler data for Magellan and PVO, the Doppler data were weighted at their intrinsic accuracy. When fitting Magellan using Doppler and differenced-Doppler data, first the Doppler data were fit. Next, the differenced-Doppler data were included, weighted at their intrinsic accuracy, and the Doppler data deweighted by an increasing factor until the root-mean-square Doppler residual increased by 10 percent over the Doppler-only case. The typical deweighting factor for the Doppler data was 10–20. This empirically derived procedure allowed the differenced-Doppler data to influence the solution without unduly weakening the Doppler data [2,3]. When fitting Doppler and SBI data for Magellan and PVO, the SBI and PVO Doppler data were weighted at their intrinsic accuracies while it was found necessary to deweight the Magellan Doppler data by a factor of 100 to allow the post-fit SBI residuals to be minimized.

The orbit solutions for Magellan using Doppler plus differenced-Doppler data were similar to the operational orbit solutions. Operational orbit determination is performed using data arcs covering twelve orbits, using X-band Doppler and differenced-Doppler data. Consecutive operational Magellan orbit solutions use overlapping data arcs with four orbits of data in common between solutions. This has provided the sub-kilometer solution-to-solution consistency needed by the radar mapping instrument [2,3].

VI. Orbit Determination Covariance

In addition to comparing successive orbit solutions to measure orbit determination accuracy, the solution-to-solution differences are compared below to a nominal orbit covariance. This orbit covariance was formed using a priori uncertainties for a number of consider parameters. Table 5 lists the a priori uncertainties assumed.

The gravity field uncertainty was a major error source for all solutions and dominated the orbit uncertainty for solutions using only Doppler data. Due to computational limitations, the considered gravity field covariance was of degree and order 6 rather than the covariance of the field of degree and order 21. A diagonal covariance of degree and order 6 was taken from a previous gravity field determination [12] scaled by an empirically determined factor of 1.5. With this assumed gravity field uncertainty, the observed solution-to-solution variations for Magellan solutions using only Doppler data approximately agreed with the considered gravity field uncertainty. The uncertainty in Venus' GM was similarly taken to be a value which gave approximately the observed variation in determination of the Magellan and PVO semi-major axes from solutions using only Doppler data. These assumptions for the gravity field uncertainty were adopted only to give an appropriate spacecraft trajectory uncertainty for solution-to-solution differences for this demonstration.

Solar pressure forces were considered with an uncertainty of 10 percent of their nominal value. The zenith ionosphere uncertainty was taken to be 10^{17}electrons/m^2 which is a typical uncertainty in the daily ionosphere calibration [7]. The zenith troposphere uncertainty was taken to correspond to 4 cm of path delay due to observed variation in water vapor content compared with the seasonal model employed.[1]

Small thruster firings occurred twice daily for Magellan to desaturate momentum wheels used to control the spacecraft attitude. The effect of these thruster firings on the spacecraft trajectory was modeled as an impulsive maneuver. The magnitude of the velocity imparted to the spacecraft from each maneuver was typically $\sim$ 3 mm/sec. Calibrations for the thruster firings are provided on the spacecraft telemetry from which the magnitude of the maneuver can be determined to a few percent [13]. The uncertainty in each maneuver was assumed to be 0.1 mm/sec.

Uncertainties in station frequency and timing standards affect station-differenced data types more strongly than single-station Doppler data. The uncertainty in station frequency calibrations was important for solutions containing differenced-Doppler data. The station frequency calibration uncertainty was assumed to be 5×10^{-14} sec/sec [14]. Uncertainties in station clock epoch were important for solutions containing SBI data. The effect of an unknown offset in the time-tags for the SBI data at the two Earth receivers is discussed in [5]. For analysis of the SBI data, nominal values for the difference in station clocks between the DSN stations were taken from Very Long Baseline Interferometry measurements made routinely for maintaining knowledge of Earth orientation.[2] The uncertainty of this determination of the station-differenced clock epoch uncertainty was 0.2 μsec.

---

[1] S. E. Robinson, "Errors in Surface Model Estimates of Zenith Wet Path Delays Near DSN Stations," JPL Interoffice Memorandum 335.4-594 (internal document), Jet Propulsion Laboratory, Pasadena, California, September 3, 1986.

[2] S. H. Oliveau, L. Sung, and J. A. Steppe, "TEMPO Group Clock Synchronization and Syntonization Report from the DSN VLBI Mark IV-85 System," JPL Engineering Memorandum 335-192 (internal document), Jet Propulsion Laboratory, Pasadena, California, February 25, 1991.

Figures 5 and 6 show the root-sum-square (rss) position covariance for Magellan and PVO at apoapsis using several combinations of data types. The rss position uncertainty is usually largest at apoapsis due to the fact that the uncertainty in determination of the longitude of the orbit ascending node with respect to the plane of the sky dominates the uncertainty in spacecraft position determination. The position uncertainty for both spacecraft when only Doppler data are included is dominated by the considered gravity field uncertainty. This is in contrast to the case for PVO when using a one-day data arc where the data noise dominated the position uncertainty and the position determination uncertainty was much larger [15]. The position determination uncertainty for Magellan using Doppler plus differenced-Doppler data contains nearly equal contributions from data noise, troposphere, clock rate, and gravity field uncertainties. The position uncertainties for solutions containing SBI data are dominated by gravity field uncertainty but at a reduced level. With the 48-hour Doppler data arc the position improvement for PVO when SBI data are included is much less than if a one-day data arc is used [15].

These orbit determination covariances are nominal only for this demonstration period, especially for data types other than SBI. No attempt has been made to optimize orbit determination performance by altering data scheduling, elevation cutoff, or different data weighting algorithms [16]. The orbit covariances are used primarily to check that the observed solution-to-solution differences are understood in terms of known mismodeled parameters.

VII. Orbit Determination Results

Figure 7 shows the rss position differences between solutions for Magellan from adjacent data arcs using only Doppler data, plotted over one orbit. The expected differences are also shown. The expected position difference curves are derived by assuming each solution is an independent sample from a distribution characterized by the formal covariance given in the previous section. Thus the expected difference between two solutions that use similar data schedules is just the position uncertainty for either solution times the square root of two. The Doppler-only solution statistics are dominated by the (considered) gravity field uncertainty. The gravity field uncertainty was determined in such a way as to get approximate agreement between the expected position difference and the actual solution differences for Doppler-only solutions for Magellan.

Figure 8 shows the rss position differences and the expected position difference for Magellan orbit solutions from adjacent data arcs using Doppler plus differenced-Doppler data. The Magellan mission requirement is for adjacent solutions to differ by less than ~1.4 km (0.15 km radial, 1 km cross-track, and 1 km down track) over the mapping period of the orbit, which is approximately the central 1-hour period shown in Figs. 7, 8, and 9.[3] It can be seen that Doppler data alone would not satisfy the mission requirements. The Doppler plus differenced-Doppler solutions generally satisfy the mission requirements (and could be improved by using overlapping data arcs as is done operationally). Note that the trajectory differences for the Doppler plus differenced-Doppler solutions are consistently less than the value expected from the covariance analysis. This implies that considering a constant zenith troposphere uncertainty of 4 cm overestimates the effect on the trajectory, possibly because the deviations from the calibrations for the two sample time periods were smaller than normal.

Figure 9 shows the orbit solution differences for Magellan solutions using Doppler plus SBI data. The Doppler plus SBI solutions are seen to be significantly better than the Doppler-only or Doppler plus differenced-Doppler solutions as expected. This is true even though the SBI data were acquired at S-band while the differenced-Doppler data were acquired at X-band. SBI data acquired at X-band are expected to be more accurate by about one order of magnitude [5].

Figure 10 shows the rss position differences and the expected position difference for PVO orbit solutions from adjacent data arcs using only Doppler data. Figure 11 shows the orbit solution differences for PVO solutions using Doppler plus SBI data. The PVO Doppler-only solution differences are much smaller than the Magellan solution differences for solutions with either Doppler-only or Doppler plus differenced-Doppler. This is due to the PVO periapsis altitude being much higher than Magellan's periapsis altitude, which makes the PVO orbit determination much less sensitive to gravity field mismodeling. The addition of SBI data only slightly improves the PVO orbit solutions because, with a two-day data arc and low sensitivity to gravity field mismodeling, the Doppler data determine the longitude of the ascending node of PVO's orbit with accuracy comparable to the SBI data.

Table 6 lists the time-averaged orbit position difference and an overall average for Magellan and PVO for each combination of data types studied. This figure of merit is introduced to quantitatively compare the orbit determination performance. Using the seven solution-to-solution

[3] S. N. Mohan, *Magellan Navigation Plan*, JPL Document 630-51, Rev. B (internal document), Jet Propulsion Laboratory, Pasadena, California, March 23, 1988.

comparisons possible for this demonstration, Table 6 indicates that orbit solutions using SBI data are significantly more accurate for Magellan and slightly more accurate for PVO. The quantitative ratios will, in general, depend on orbit geometry, data arcs, and estimation strategy.

VIII. Conclusion

Orbit determination results have been obtained for Pioneer Venus Orbiter and Magellan using same-beam interferometry data, which is a new data type for planetary orbiter navigation. The orbit determination accuracy using this data type, based on solution-to-solution consistency, has been explained in terms of nominal error models. For the particular orbit determination strategy and observational geometry used for this limited data set, the orbit determination accuracy for Magellan using SBI in combination with two-way Doppler data is better by a factor of four than orbit determination accuracy using two-way Doppler plus differenced-Doppler data and better by a factor of eighteen than orbit determination accuracy using Doppler alone. This new data type should find much application in the future as more missions with multiple orbiters and/or landers are flown to Mars.

Acknowledgments

The authors thank Doug Engelhardt of the Magellan navigation team and Neil Mottinger of the Pioneer Venus Orbiter navigation team for their assistance in spacecraft modeling.

References

[1] S. R. Poole, M. P. Ananda, and C. E. Hildebrand, "Radio Interferometric Measurements for Accurate Planetary Orbiter Navigation," in *AAS Advances in the Astronautical Sciences*, vol. 40, part 1, pp. 93–111, San Diego, California: Univelt Inc., 1980.

[2] D. B. Engelhardt, J. B. McNamee, S. K. Wong, F. G. Bonneau, E. J. Graat, R. J. Haw, G. R. Kronschnabl, and M. S. Ryne, "Determination and Prediction of Magellan's Orbit," paper AAS-91-180, presented at the AAS/AIAA Spaceflight Mechanics Meeting, Houston, Texas, February 11–13, 1991.

[3] J. D. Giorgini, E. J. Graat, T.-H. You, M. S. Ryne, S. K. Wong, and J. B. McNamee, "Magellan Navigation Using X-Band Differenced Doppler During Venus Mapping Phase," paper AIAA-92-4521, presented at the AIAA/AAS Astrodynamics Conference, Hilton Head, South Carolina, August 10–12, 1992.

[4] W. M. Folkner and J. S. Border, "Orbiter–Orbiter and Orbiter–Lander Tracking Using Same-Beam Interferometry," *The Telecommunications and Data Acquisition Progress Report 42-109*, vol. January–March 1992, Jet Propulsion Laboratory, Pasadena, California, pp. 74–86, May 15, 1992.

[5] J. S. Border, W. M. Folkner, R. D. Kahn, and K. S. Zukor, "Precise Tracking of the Magellan and Pioneer Venus Orbiters by Same-Beam Interferometry, Part I: Data Accuracy Analysis," *The Telecommunications and Data Acquisition Progress Report 42-110*, vol. April–June 1992, Jet Propulsion Laboratory, Pasadena, California, pp. 1–20, August 15, 1992.

[6] C. C. Chao, *The Troposphere Calibration Model for Mariner Mars 1971,* JPL Technical Report 32-1587, Jet Propulsion Laboratory, Pasadena, California, pp. 61–76, March 1974.

[7] H. N. Royden, D. W. Green, and G. R. Walson, "Use of Faraday-Rotation Data from Beacon Satellites to Determine Ionospheric Corrections for Interplanetary Spacecraft Navigation," *Proceedings of the Satellite Beacon Symposium*, edited by A. W. Wernik, Warszawa, Poland, pp. 345–355, May 1980.

[8] J. B. McNamee, G. R. Kronschnabl, S. K. Wong, and J. E. Ekelund, "A Gravity Field to Support Magellan Navigation and Science," *J. Astron. Sci.*, vol. 40, pp. 107–134, 1992.

[9] M. E. Davies, T. R. Colvin, P. G. Rogers, P. W. Chodas, W. L. Sjogren, E. L. Akim, V. A. Stepanyantz, Z. P. Vlasova, and A. I. Zakharov, "The Rotation Period, Direction of the North Pole, and Geodetic Control Network of Venus," *J. Geophys. Res.*, vol. 97, pp. 13,141–13,151, 1992.

[10] G. J. Bierman, *Factorization Methods for Discrete Sequential Estimation*, San Diego, California: Academic Press, 1977.

[11] G. M. Keating, J. L. Bertaux, S. W. Bougher, T. E. Cravens, R. E. Dickinson, A. E. Hedin, V. A. Krasnopolsky, A. F. Nagy, J. Y. Nicholson III, L. J. Paxton, and U. von Zahn, "Model of Venus Neutral Upper Atmosphere: Structure and Composition," *Adv. Space Res.*, vol. 5, pp. 117–171, 1985.

[12] N. A. Mottinger, W. L. Sjogren, and B. G. Bills, "Venus Gravity: A Harmonic Analysis and Geophysical Implications," *J. Geophys. Res.*, vol. 90, supplement, pp. C739–C756, February 15, 1985.

[13] D. B. Engelhardt and S. N. Mohan, "Deterministic Errors in the Magellan Orbit Due to Attitude Control Thruster Activity," paper AIAA-89-0349, presented at the 27th Aerospace Sciences Meeting, Reno, Nevada, January 9–12, 1989.

[14] P. A. Clements, A. Kirk, and R. Unglaub, "Results of Using the Global Positioning System to Maintain the Time and Frequency Synchronization in the Deep Space Network," *The Telecommunications and Data Acquisition Progress Report 42-89*, vol. January–March 1987, Jet Propulsion Laboratory, Pasadena, California, pp. 67–72, May 15, 1987.

[15] W. M. Folkner, D. B. Engelhardt, J. S. Border, and N. A. Mottinger, "Orbit Determination for Magellan and Pioneer 12 Using Same-Beam Interferometry," paper AAS 91-393, presented at the AAS/AIAA Astrodynamics Specialist Conference, Durango, Colorado, August 19–22, 1991.

[16] J. S. Ulvestad, "Orbit-Determination Performance of Doppler Data for Interplanetary Cruise Trajectories, Part II: 8.4 GHz Performance and Data-Weighting Strategies," *The Telecommunications and Data Acquisition Progress Report 42-108*, vol. October–December 1991, Jet Propulsion Laboratory, Pasadena, California, pp. 49–65, February 15, 1992.

Table 1. Spacecraft orbital elements with respect to the plane-of-sky on February 16, 1991.

Element	Magellan	PVO
Semimajor axis, km	10425.0	39453.4
Eccentricity	0.39287	0.81985
Inclination, deg	38.301	122.99
Argument of perigee, deg	74.797	88.513
Longitude of ascending node, deg	−15.387	−41.412
Time past periapsis, sec	−5830.6	−43194
Epoch	12:06:00	13:36:04
Periapsis altitude, km	278	1056

Table 2. Spacecraft orbital elements with respect to the plane-of-sky on April 6, 1991.

Element	Magellan	PVO
Semimajor axis, km	10425.0	39450.8
Eccentricity	0.39307	0.82352
Inclination, deg	22.541	65.005
Argument of perigee, deg	−83.371	103.64
Longitude of ascending node, deg	147.50	−30.623
Time past periapsis, sec	−5866.8	−43183
Epoch	12:45:15	13:25:13
Periapsis altitude, km	278	1056

Table 3. Data coverage for SBI demonstration.

Solution	February 1991			
	13–16	16–18	18–20	20–22
PVO start time	Feb. 13, 13:36	Feb. 16, 13:36	Feb. 18, 13:36	Feb. 20, 13:36
Magellan start time	Feb. 14, 14:27	Feb. 16, 12:05	Feb. 18, 12:59	Feb. 20, 13:52
Data stop time	Feb. 16, 12:05	Feb. 18, 12:59	Feb. 20, 13:36	Feb. 22, 11:42
PVO Doppler, hr	11.3	13.4	16.3	11.9
Magellan Doppler, hr	24.8	26.0	26.0	25.2
Magellan differenced-Doppler, hr	6.2	6.0	5.0	5.0
SBI, hr	1.0	2.6	2.2	1.0

Table 4. Data coverage for SBI demonstration.

Solution	April 1991				
	6–8	8–10	10–12	12–14	14–16
PVO start time	April 6, 13:25	April 8, 13:24	April 10, 13:24	April 12, 13:23	April 14, 13:22
Magellan start time	April 6, 12:45	April 8, 10:23	April 10, 11:16	April 12, 12:10	April 14, 13:04
Data stop time	April 8, 10:23	April 10, 11:16	April 12, 12:10	April 14, 13:04	April 16, 13:30
PVO Doppler, hr	23.7	22.6	16.6	13.9	20.1
Magellan Doppler, hr	21.1	25.6	25.3	26.2	23.6
Magellan differenced-Doppler, hr	3.2	6.3	6.8	8.9	8.4
SBI, hr	1.4	1.7	3.9	3.0	1.7

Table 5. Assumptions for orbit determination covariance analysis.

Unadjusted parameters	A priori uncertainty
Solar pressure	10 percent of nominal value
Magellan thruster firing	0.1 mm/sec
Venus gravitational mass	0.07 km^3sec^{-2}
Venus gravity field	Diagonal covariance for terms to degree and order 6 from [12] scaled by 1.5
Zenith troposphere	4 cm
Zenith ionosphere	10^{17} electrons/m^2
Station clock rate	5×10^{-14}
Station-differenced clock epoch	0.2 μsec

Table 6. Time-averaged position differences for Magellan and PVO using only Doppler data, Doppler plus differenced-Doppler data, or Doppler plus SBI data.

Data	RSS position difference for Magellan, km	RSS position difference for PVO, km
Doppler only	4.35	0.32
Doppler plus differenced-Doppler	0.97	–
Doppler plus SBI	0.24	0.23

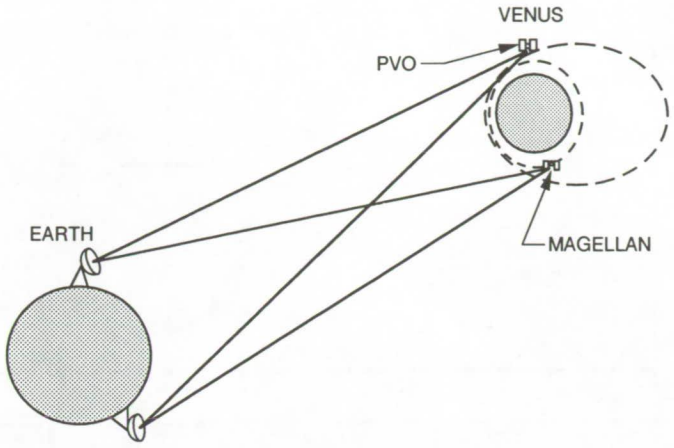

Fig. 1. Same-beam interferometry measurement technique.

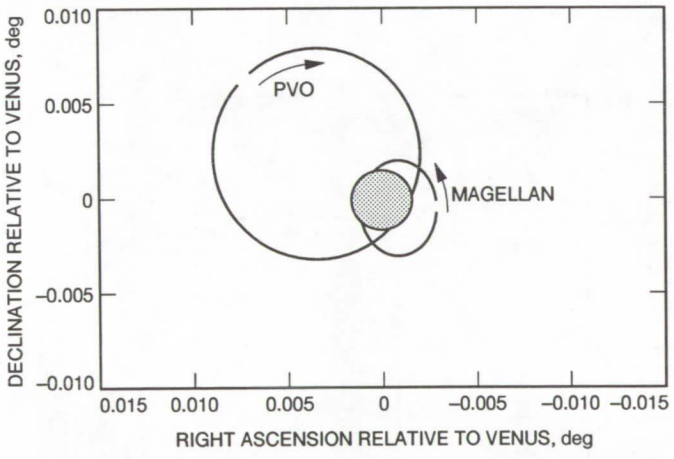

Fig. 2. Magellan and PVO orbits about Venus as seen from Earth on February 16, 1991.

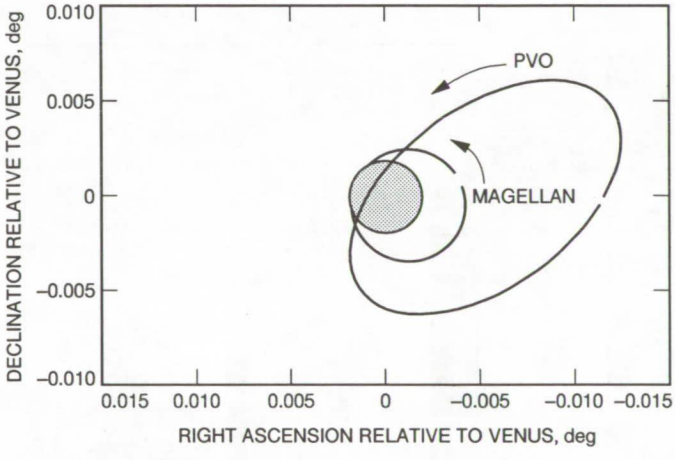

Fig. 3. Magellan and PVO orbits about Venus as seen from Earth on April 6, 1991.

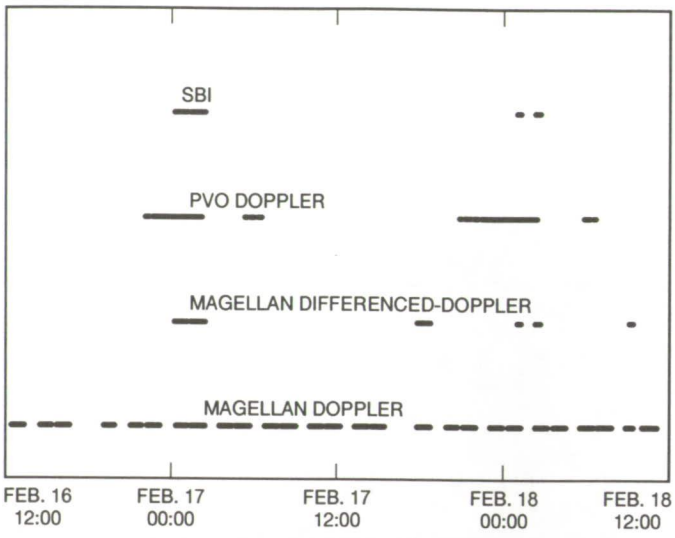

Fig. 4. Typical 48-hour data schedule for Magellan and PVO.

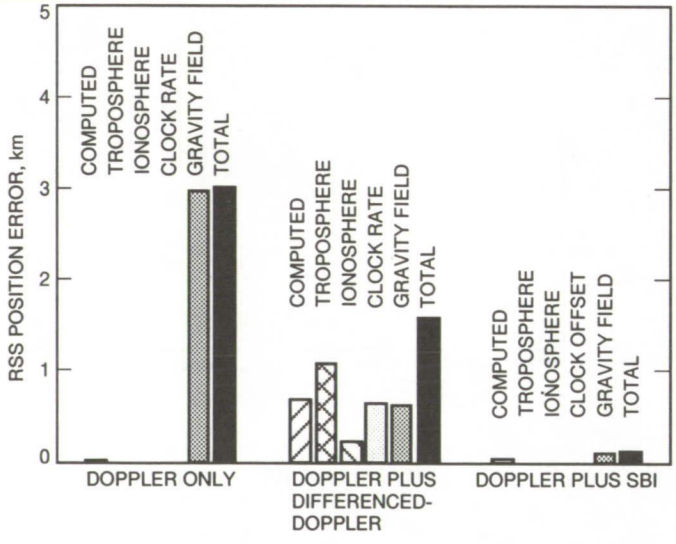

Fig. 5. Magellan position uncertainty at apoapsis using various combinations of data. Contributions from solar pressure and maneuver uncertainties are negligible and are not shown.

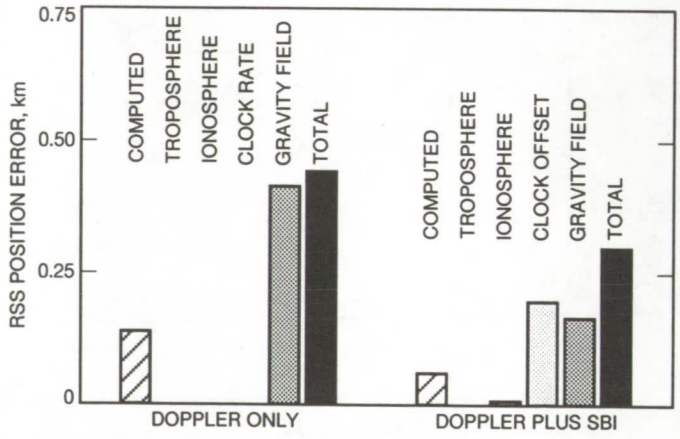

Fig. 6. PVO position uncertainty at apoapsis using various combinations of data. Contribution from solar pressure uncertainty is negligible and is not shown.

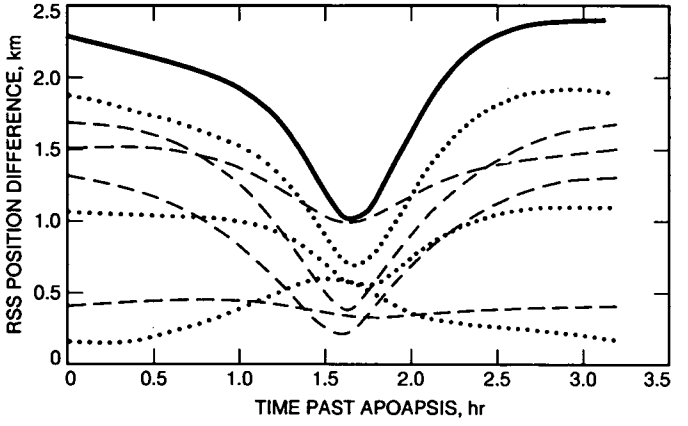

Fig. 7. Magellan solution-to-solution trajectory differences using only Doppler data. The dashed curves are for solutions in February 1991. The dotted curves are for solutions in April 1991. The dark solid curve is the expected trajectory difference based on the covariance analysis.

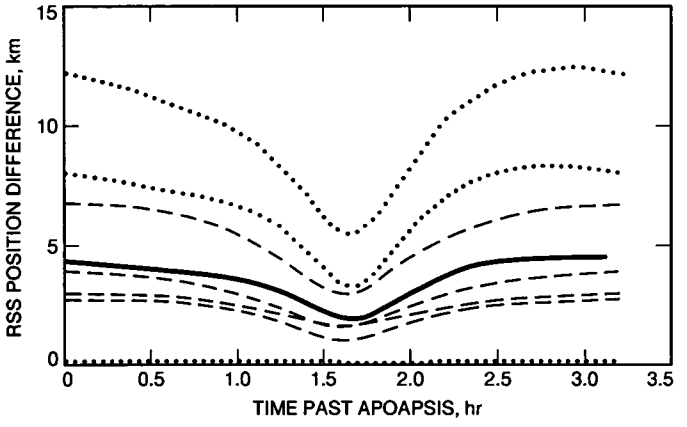

Fig. 8. Magellan solution-to-solution trajectory differences using Doppler plus differenced-Doppler data. The dashed curves are for solutions in February 1991. The dotted curves are for solutions in April 1991. The dark solid curve is the expected trajectory difference based on the covariance analysis.

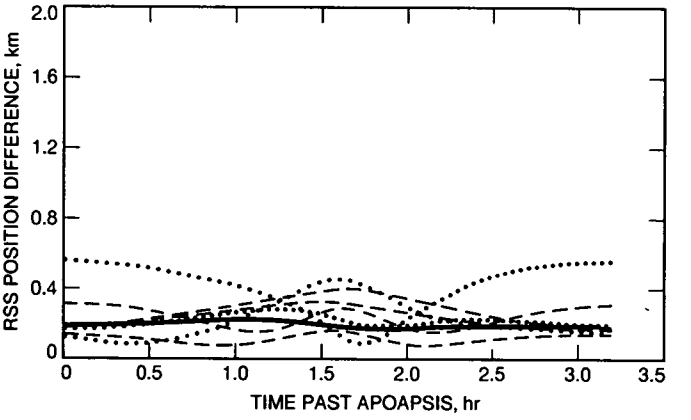

Fig. 9. Magellan solution-to-solution trajectory differences using Doppler plus SBI data. The dashed curves are for solutions in February 1991. The dotted curves are for solutions in April 1991. The dark solid curve is the expected trajectory difference based on the covariance analysis.

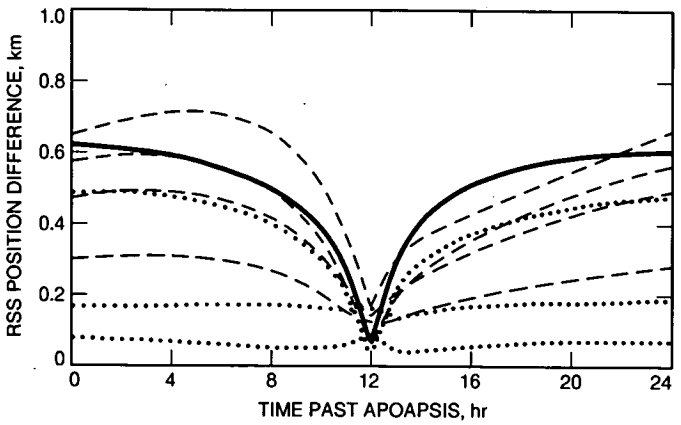

Fig. 10. PVO solution-to-solution trajectory differences using only Doppler data. The dashed curves are for solutions in February 1991. The dotted curves are for solutions in April 1991. The dark solid curve is the expected trajectory difference based on the covariance analysis.

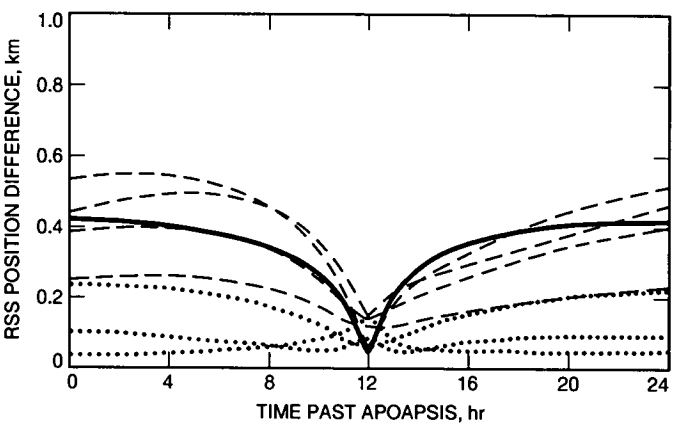

Fig. 11. PVO solution-to-solution trajectory differences using Doppler plus SBI data. The dashed curves are for solutions in February 1991. The dotted curves are for solutions in April 1991. The dark solid curve is the expected trajectory difference based on the covariance analysis.